



## Full Length Article

# A low energy consumption sono-microreactor for regeneration of MEA and MEA/AMP solutions



Hamed Rashidi\*, Maryam Dehbani, Mahyar Amiri

Chemical Engineering Department, Kermanshah University of Technology, Kermanshah, Iran

## ARTICLE INFO

**Keywords:**  
CO<sub>2</sub> desorption  
MEA solution  
Ultrasound  
Acoustic cavitation  
Microchannel

## ABSTRACT

Ultrasound was applied to a microreactor for CO<sub>2</sub> desorption from 30 wt% aqueous amine solutions. The ultrasonic transducer was attached directly to the microchannel in order to achieve the greatest ultrasound irradiation by the solution. The behavior of two-phase flow was assessed by a digital microscope camera, illustrating the formation of gas bubbles and its growing through the microchannel reactor. Effects of MEA concentration, solution flow rate, temperature, and ultrasonic wave's power on the desorption rate and desorption percentage was evaluated. Desorption percentage showed a direct relationship with temperature, ultrasound power, and concentration of MEA solution but an inverse relationship with the flow rate. In addition to performing the regeneration process at lower temperatures than required by traditional procedures which can reduce solvent damage, 50 % energy saving was obtained using the designed contactor. In the next step, aqueous blended AMP/MEA solutions with two different ratios were assessed. For a 20 wt% AMP + 10 wt% MEA solution at 0.25 mL/min, an energy saving of about 62 % was achieved as compared to the conventional method's benchmark of 30 wt% MEA.

## Introduction

Climate change has raised many concerns in recent years. To halt global warming, researchers are seriously looking for ways to reduce the emissions of the greenhouse gasses, the most important of which is carbon dioxide [1,2].

The use of fossil fuel is responsible for 83 % of anthropogenic greenhouse gas emissions and it is expected to increase considerably in the not too distant future. To comply with the standards requirements, it is critical to use proper combustibility gas purification technologies, particularly post-combustion CO<sub>2</sub> capture. [3,4].

The most reliable and widely used post-combustion carbon dioxide capture (PCCC) is amine-based chemical absorption methods [5,6]. However, some restrictions apply to CO<sub>2</sub> removal utilizing an amine-based solution. One of the significant challenges for chemical absorption of CO<sub>2</sub> using alkanolamines is the high energy usage for solvent regeneration [7,8]. At greater temperatures, where the potential of solvent degradation increases, desorption energy consumption is reduced. [9]. Solvent degradation is known as another disadvantage of CO<sub>2</sub> capture technology using amines. In addition to corrosion, amine loss and generation of volatile compounds, amine degradation results in

higher total CO<sub>2</sub> capture cost [10]. Temperature is the primary cause of thermal degradation which is occurred in the desorption process from chemical solvents [9]. Therefore, low-temperature solvent regeneration can reduce the rate of degradation and solvent make-up. [9]. Many efforts have been made to improve the performance of the regeneration process and reduce the energy demand. The employment of alternative solvents is one of the most prevalent approaches [11,12]. Some examples include the blends of amines [13], hybrid solvents [14,15], modern amine-based solvents like diamines [16], ionic liquids [17,18], and sterically hindered amines such as 2-amino-2-methyl-1-propanol (AMP).

One of the most effective ways to enhance the CO<sub>2</sub> capture techniques is to find an appropriate liquid-gas contactor, which could intensify the heat and mass transfer as result of contact area increase and consequently, decrease the required consumption energy. A recent development in the mass transfer contactors is the use of various types of microreactors [19]. Different effective flow patterns may be induced inside a microchannel, in which two immiscible fluids are flowing, depending on the operating conditions and fluids properties [20,21]. In recent decades, interest in utilizing microchannel reactors as an efficient two-phase contactor has been continuously increasing due to their distinctive benefits include a short diffusion length, a wide two-phase contact surface per unit volume, improved mixing outcome, and hence

\* Corresponding author.

E-mail address: [h\\_rashidi@kut.ac.ir](mailto:h_rashidi@kut.ac.ir) (H. Rashidi).

## Nomenclature

C	Molar concentration, $kmol/m^3$
DP	Desorption percentage, %
J	$CO_2$ desorption rate, $kmol/s$
m	Mass, kg
Q	Volume flow rate, $m^3/s$
q	Energy, J
Greek letters	
$\alpha$	$CO_2$ loading of the amine solution, $mol CO_2/mol MEA$

## Subscript

$CO_2$	Carbon dioxide
des	Desorption
in	Microchannel inlet
L	Liquid phase
out	Microchannel outlet
US	Ultrasound

higher heat and mass transfer [22].

Some scholars have studied the beneficial effect of employing microchannel reactors on boosting the efficiency of  $CO_2$  capture processes in terms of absorption and desorption [23–25]. Compared to absorption, the  $CO_2$  stripping method is more complicated, because it incorporates heat transfer in addition to gas–liquid mass transfer. [26].

Liu et al. [26] examined  $CO_2$  removal from N-methyldiethanolamine (MDEA) solutions in a straightforward microreactor built utilizing the micromatching method. They came to the conclusion that the rate of  $CO_2$  removal was most sensitive to desorber temperature among other parameters such as concentration of MDEA solution,  $CO_2$  loading, and solution flow rate. They demonstrated the efficient  $CO_2$  desorption using microreaction so that the state of equilibrium occurred during the solution residence time of 7 s. They observed that the mass transfer coefficient of stripping tests was significantly greater than that of traditional techniques. In a subsequent investigation employing their previous system [27], they also determined the energy demand and heat transfer characteristics of  $CO_2$  stripping from loaded MDEA solution. Nucleate boiling proved to be the primary mode of heat transfer, while stripping temperature was shown to have the greatest impact on heat flux.

Utilizing ultrasonic waves is another cutting-edge method that has proven to be effective for enhancing the  $CO_2$  desorption process. Ultrasound is the mechanical waves with frequency higher than 20 kHz [28]. Acoustic cavitation is the predominant phenomenon caused by the propagation of power ultrasound inside a liquid medium. When the local pressure reduced enough to overcome the intermolecular forces, gas bubbles are generated. [29,30]. These cavitation bubbles oscillate, grow or join together and finally implode violently, having consequences including physical, chemical and heat effects. Micro-streaming, micro-jets and shock waves are some significant physical effects induced by ultrasonication [31].

All of these effects cause the liquid's micro-scale turbulence to grow and hence increase heat and mass transfer [32,33]. the acoustic cavitation which is dominant in low frequency ultrasound is proven the main factor for the desorption enhancement [34]. Since just a small portion of the overall ultrasound energy comes from thermal effects, ultrasound does not dramatically raise the fluid's temperature. This feature of ultrasound can cause solvent regeneration at low temperature, which reduces the solvent damage. Accordingly, applying ultrasound to the  $CO_2$  desorption process can improve the efficiency and also provide the possibility of performing the process at low temperatures.

Gantert and Moller [35] have utilized 25 kHz and 37.5 kHz ultrasound in both batch and continuous desorption reactor. They found that

by using ultrasound vibrations,  $CO_2$  desorption from aqueous amine solutions could be accomplished at temperatures lower than 80 °C. The use of ultrasound irradiation with frequency of 28 kHz for  $CO_2$  separation from MEA-water solutions at 25 °C was investigated by Tanka et al. [36]. According to the findings, ultrasonic irradiation considerably increased the rate of  $CO_2$  removal from low-concentration MEA solution when compared to stirring. They also concluded that decrease in the concentration of MEA solutions resulted in increased  $CO_2$  desorption rate. Ultrasound effects on the enhancement of  $CO_2$  desorption from rich MEA-water solutions in a reboiler at the laboratory level was studied by Ying et al. [37]. Temperature, flow rate,  $CO_2$  loading, ultrasound frequency, and ultrasound power were the factors whose impacts were assessed. The use of ultrasonic irradiation led to 400 % improvements in  $CO_2$  removal and a 36 % reduction in energy consumption when compared to processes that simply used heat. Employing Aspen In-plant Cost Estimator and Aspen Plus, they also carried out the cost assessment for industrial instances including the use of ultrasonic propagations, resulting in a 19 % cost saving [38].

Based on the above discussions, positive effects of both microfluidic systems and ultrasonication on enhancement of heat and mass transfer, and consequently on  $CO_2$  desorption improvement has been proven. The literature has discussed the benefits of employing ultrasonic waves in multi-phase flow microfluidic systems. [39–41].

Given the advantages of each of the two techniques for mass transfer improvement as well as synergistic effect of two methods [42], in this study, an ultrasound-equipped micro-reactor was used for  $CO_2$  stripping process. A low frequency ultrasonic transducer in proximity with a micro-reactor without the existence of a liquid, as the propagation medium, was designed and fabricated. First, to evaluate the performance of designed contactor in  $CO_2$  stripping process, MEA which is known as the benchmark solvent was utilized. The effects of MEA concentration, flow rate of aqueous MEA solution, temperature, and ultrasound power amplitude on stripping process and its corresponding consumption energy were investigated. In the next step,  $CO_2$  desorption from aqueous blends of 2-amino-2-methyl-1-propanol (AMP) and MEA was also assessed.

## Experimental

### Materials

MEA was supplied from Shazand Arak Petrochemical Company, Iran with a purity of 99 % with no further purification. The MEA solution was prepared by the use of double-distilled water in the range of 10 to 30 wt %. AMP and HCl were purchased from Merck-Schuchardt. As the pH indicator in the titration process, methyl orange from the French Bio-Chem Company was purchased. From Balon Gas, 99.99 % pure  $CO_2$  gas was provided.

### Design of ultrasound-equipped microreactor

As depicted in Fig. 1, a novel sono-microreactor was designed and constructed. In this contactor ultrasound transducer and microchannel reactor were in the direct contact between and no liquid medium was employed for transmitting the waves to the microchannel. For this purpose, a 6 × 6 cm plate was mounted on a 28 kHz, 100 W ultrasound transducer. The dimensions of the plate were determined by the transducer's diameter, which was 5.8 cm. Considering that the ultrasound transducer's contact area was built of aluminum, the plate was also chosen from the same material in order to prevent attenuation of the ultrasound. The thickness of the aluminum plate was 4 mm. To insert the tube, four parallel slots with a 2.7 mm square cross-section were drilled in the plate. Embedding the microchannel inside a thick aluminum plate caused more uniform emission of ultrasound wave to the passing solution. As a flexible, chemically passive and transparent material to have a clear vision of fluid flowing inside, Perfluoroalkoxy copolymer (PFA)

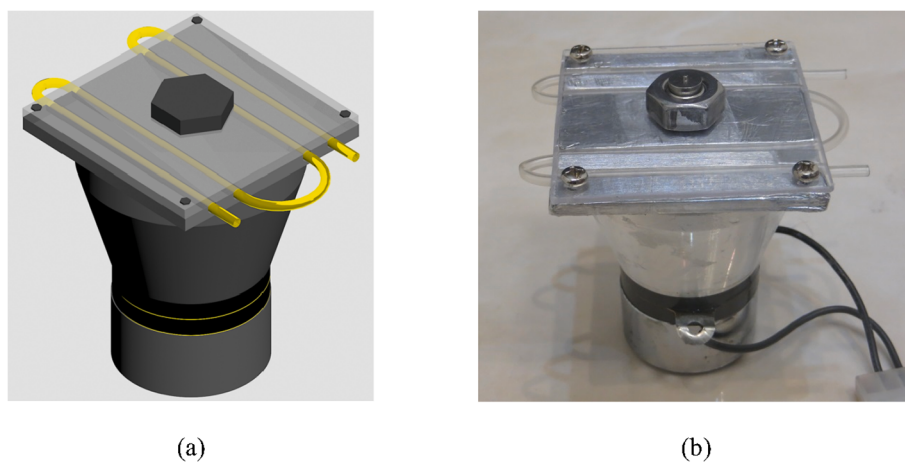


**Fig. 1.** Designed contactor (a) Schematic view, (b) Photo.

was employed for tubing. The inner and outer radius of the tube were 0.8 mm and 1.35 mm, respectively, and it is kept in place by a 3 mm thick poly methyl methacrylate (PMMA) cover plate. PMMA was chosen due to being transparent, with the possibility of shooting from two-phase fluid, as well as avoiding damage caused by the ultrasonic exposure.

#### Procedure

In Fig. 2, the laboratory's setup is schematically illustrated. In the first step, MEA was considered as a benchmark chemical solvent to evaluate the desorption process. Three different concentrations of MEA solution were examined: 10, 20, and 30 wt%. After preparing the MEA solution, it was transferred into a CO<sub>2</sub> loading tank. The solution then was given sufficient time until it reached CO<sub>2</sub> saturation. It is proven that the higher rate of CO<sub>2</sub> stripping from amine-based solutions with a specific concentration is obtained for the one with higher CO<sub>2</sub> loading due to the greater driving force of mass transfer [26,37]. So, CO<sub>2</sub>-saturated solutions were studied in the present study. The corresponding CO<sub>2</sub> loadings of 10, 20, and 30 wt% MEA solutions were 0.63, 0.59, and 0.50  $\frac{molCO_2}{molMEA}$ , respectively. The acidification titration procedure described by the AOAC (Association of Official Analytical Chemists) was used to determine the CO<sub>2</sub> loading of MEA solution [43]. Briefly, for the CO<sub>2</sub> loading measurement, 1 M HCl was added into a 1 mL MEA solution sample until neutralization took place. The amount of CO<sub>2</sub> emitted by

the reaction was equal to the displaced volume of the deionized water inside the gas burette.

An excess amount of HCl was also used to achieve a thorough release of CO<sub>2</sub>. The height changes of the liquid inside the gas burette minus the total volume of HCl added equals the CO<sub>2</sub> gas content of the solution. Considering CO<sub>2</sub> as an ideal gas, the CO<sub>2</sub> loading ( $\alpha = \frac{n_{CO_2}}{n_{amine}}$ ) was determined.

CO<sub>2</sub>-loaded MEA solution at 55, 65, 75, and 85 °C was delivered into the tubing using a peristaltic pump. Notably, the test section was insulated during the experiments. Varying ultrasonic power amplitudes were applied to the flowing solutions inside the microreactor at varying flow rates. At the microreactor's output, a condenser was placed to collect condensable components and maintain the MEA solution's concentration. Finally, the outlet solution was once again examined for the purpose of measuring the CO<sub>2</sub> loading using the previously described technique.

After ensuring the high efficiency of the designed sono-microreactor and determining the optimum conditions, aqueous AMP/MEA solution with different blending ratios were evaluated. Methods of CO<sub>2</sub> absorption, experiment and analysis was the same as mentioned above.

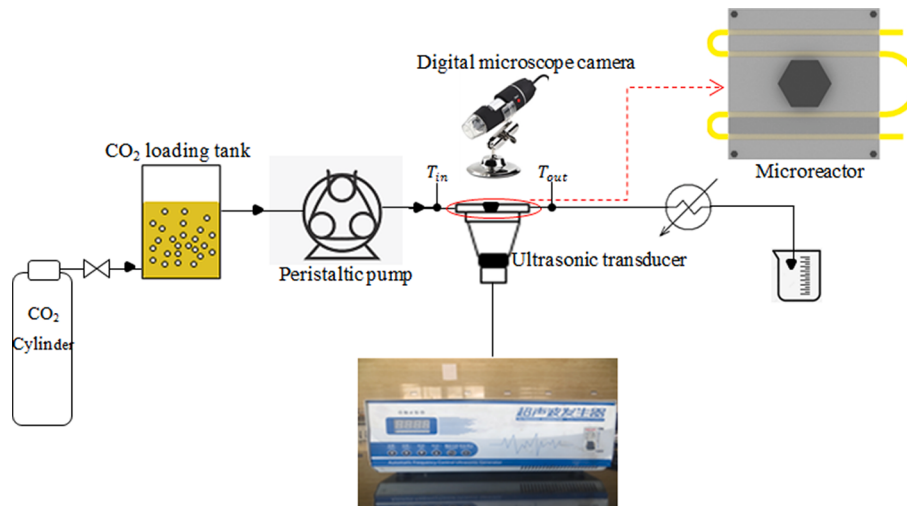


**Fig. 2.** Schematic of experimental setup.

## Theory

### Chemical reactions

$\text{CO}_2$  releases from the primary alkanolamines under the following chemical equations. Carbamate is converted to carbon dioxide through the following reaction:



According to the reaction (1),  $\text{CO}_2$  absorption capacity for MEA solution is 0.5 mol  $\text{CO}_2$ /mol MEA. The carbamate resulting from the reaction of MEA is stable; however, the produced carbamate from the reaction of AMP is unstable and undergoes the following reaction [44]:



According to the reaction (2),  $\text{CO}_2$  loading for AMP is 1 mol  $\text{CO}_2$ /mol AMP.

Some other reactions may also occur in the medium. Water after ionization reacts with bicarbonate and produces carbon dioxide:



Some produced bicarbonate reacts according to the following reactions:



The  $\text{CO}_2$  generated by chemical reactions moves into the gas phase.



### Introducing the responses

#### Desorption rate

The following equation was obtained for the desorption rate using the mass balance on the  $\text{CO}_2$  component.  $J_{\text{CO}_2}$ (desorption rate) is an expressive of the mole number of removed carbon dioxide per unit of time:

$$J_{\text{CO}_2} = Q_L C_{\text{solvent}} (\alpha_{\text{in}} - \alpha_{\text{out}}) \quad (7)$$

#### Desorption percent

The Desorption percent (DP) was calculated using the relationship below:

$$DP = \frac{\alpha_{\text{in}} - \alpha_{\text{out}}}{\alpha_{\text{in}}} \times 100 \quad (8)$$

$\text{CO}_2$  loading of aqueous amine solution ( $\alpha_{\text{CO}_2}$ ) was calculated at the input and output of the tubing.

#### Energy demand

The following formula was utilized for computing the amount of energy consumed for desorbing unit mass of carbon dioxide ( $E_{\text{des}}$ ) [5]:

$$E_{\text{des}} = \frac{P_{\text{fluid}}}{\dot{m}_{\text{CO}_2}} \quad (9)$$

Where  $P_{\text{fluid}}$  denotes the amount of power gained by the fluid during ultrasound propagation and was determined using the calorimetric method [45]. For this purpose, degassed water was used. It is worth mentioning that deionized and degassed water was chosen as an excellent sonication medium for calorimetric study in many previous studies [5,46,47]. Performing calorimetric method with degassed water causes the ultrasound energy to spend on temperature rise of the solution only, so it is simply possible to estimate the total energy delivered to the passing liquid:

$$P_{\text{fluid}} = Q_L \rho_L C_p \Delta T \quad (10)$$

$\dot{m}_{\text{CO}_2}$  denotes the mass of carbon dioxide removed from the amine solution per unit of time and was calculated by the following formula:

$$\dot{m}_{\text{CO}_2} = Q_L C_{\text{solvent}} M_{\text{CO}_2} (\alpha_{\text{in}} - \alpha_{\text{out}}) \quad (11)$$

## Results and discussions

### Two-phase behavior of $\text{CO}_2$ stripping process

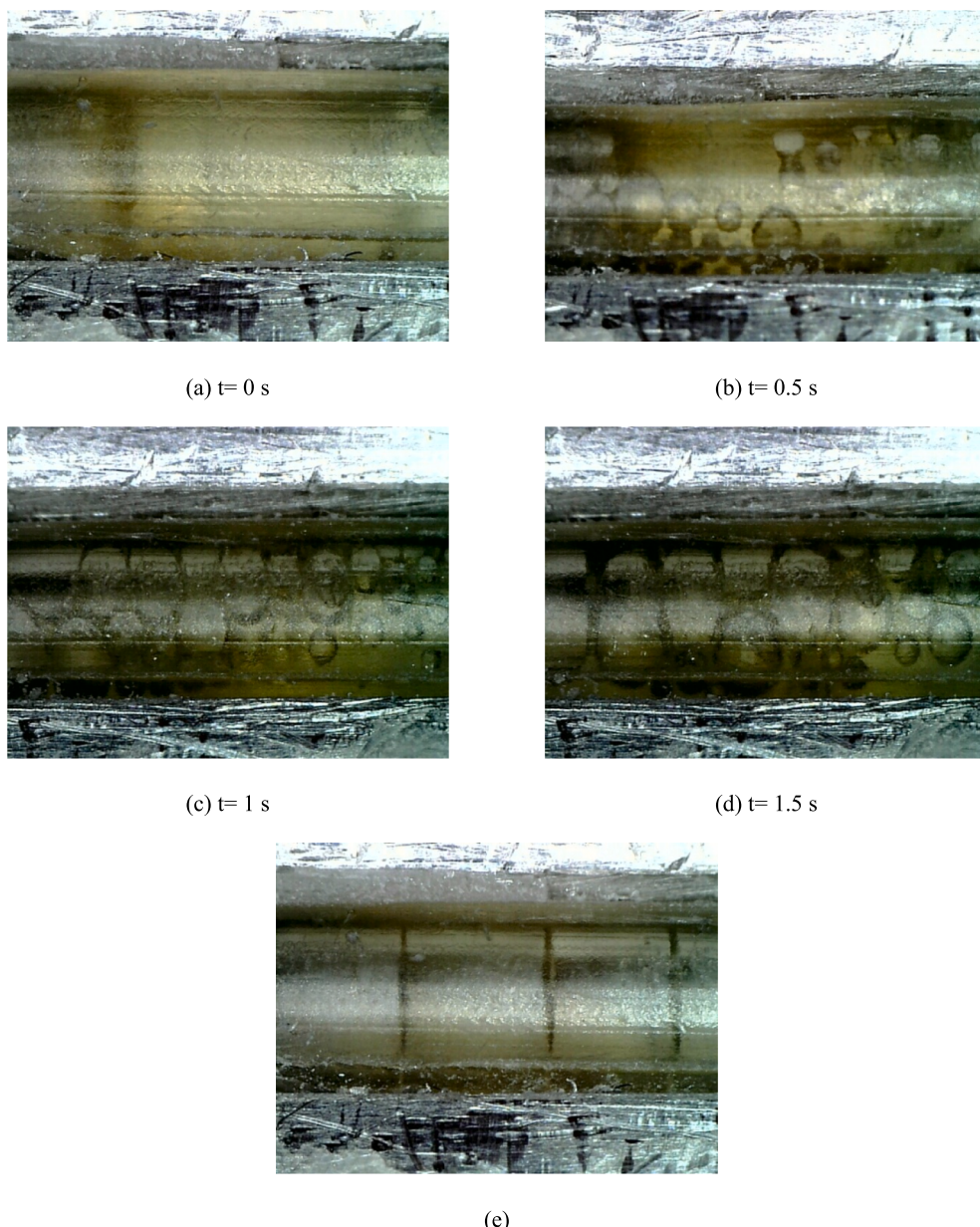
In this study, the behavior of gas–liquid flow in the process of  $\text{CO}_2$  stripping from MEA solution through the microreactor under irradiation of ultrasonic waves was also investigated. The insulation was removed from the microchannels to be able to take pictures. Acoustic cavitation is a predominant phenomenon at the frequency employed in the present investigation. Some of produced ultrasonic cavitation bubbles serve as the gas phase nuclei and thereby enhance mass transfer. Multiple mechanisms exist for cavitation bubbles to improve  $\text{CO}_2$  removal from the MEA solution. Within the liquid media, acoustic bubbles are created by negative pressure induced due to the acoustic vibrations, hence the cavitation bubbles contain substantial amount of  $\text{CO}_2$  gas. Additionally, cavitation bubbles can supply the energy needed for  $\text{CO}_2$  to move from the liquid to the gas phase through increased kinetic energy caused by size fluctuation and particularly collapse. The implosion of acoustic cavitation bubbles induces turbulence inside the fluid medium, so it can enhance the mass transfer as explained in the previous sections. These effects together with the beneficial impacts of microfluidic on increasing two-phase contact surface may lead to upgraded performance of the present contactor.

Fig. 3 demonstrates the gas–liquid two phase flow characteristics of  $\text{CO}_2$  removal from 30 wt% MEA solutions at minimum flow rate and maximum ultrasound power near the inlet of the microchannel over time (a-d) and at the outlet (e).

As is clear from Fig. 3(b), firstly numerous cavitation bubbles were generated at the vicinity of the microchannel wall where was in direct contact with ultrasound vibrations. As explained above, these bubbles could be considered as nucleation site. The flowing  $\text{CO}_2$ -rich MEA solution rapidly received ultrasonic energy and consequently increased-energy  $\text{CO}_2$  molecules immigrated from liquid to the gas phase. Due to excellent performance of the contactor in heat and mass transfer mentioned above, the bubbles containing  $\text{CO}_2$  grew up rapidly and formed the coarse bubbles as shown in Fig. 3(c). Afterward, continued mass transfer on the one hand and the unifying two or more bubble on the other hand led to formation of gas bubbles with larger size until the diameter of the bubbles was equal to the diameter of the cross section of the channel. Due to driving force of the liquid at the downstream side, the gas bubbles started passing rapidly through the microchannel. The length of  $\text{CO}_2$  bubbles continuously increased along the microchannel reactor due to mass transfer between two phases. Fig. 3(e) indicates the two-phase flow at the outlet of the microchannel reactor, clarifying that the significant amount of  $\text{CO}_2$  was separated from the MEA solution.

### Parametric analysis

In this study, the influence of some parameters on the  $\text{CO}_2$  stripping process was evaluated. Aqueous MEA solution with various concentrations of 10, 20 and 30 wt% in the  $\text{CO}_2$ -saturated condition was used. Desorption process was studied in temperature range of 55–85 °C with the interval of 10 °C. The flow rate of rich aqueous MEA solution was set in the range from 0.25 to 1.75 mL/min, with the assurance that the solution has enough time for exposing ultrasonic irradiation. The ultrasound power amplitude was studied in the range of 40–100 %.



**Fig. 3.** Flow characteristics of  $\text{CO}_2$  desorption from 30 wt% MEA solution with flow rate of 0.25 mL/min and maximum ultrasonic power amplitude: (a-d) near the inlet over the time; (e) at the outlet of the microchannel.

#### The effect of MEA concentration and flow rate

The effects of flow rate and concentration of MEA solution on  $\text{CO}_2$  desorption process were investigated. For different concentrations of MEA solution, the  $\text{CO}_2$  desorption rate versus the flow rate at 85 °C was depicted in Fig. 4.

At higher MEA solution flow rates when greater amount of loaded MEA solution flowed in the microchannel, more  $\text{CO}_2$  had the potential to be released. Accordingly, Fig. 4 correctly illustrated increased the rate of desorption with increasing MEA solution flow rate at various concentrations. This is consistent with the results presented by Liu et al. [26].

The rate of  $\text{CO}_2$  desorption and MEA solution flow were almost linearly related, however the desorption rate at the lowest MEA concentration only offered a small enhancement with flow rate. At higher concentration of MEA solution, desorption rate was more sensitive to flow rate changes so that the slope of the desorption rate versus flow rate for 30 wt% MEA solution compared to 10 wt% MEA solution was almost 3 times.

Desorption percent, unlike desorption rate, showed a decrease with

increasing MEA solution flow rate as observed in Fig. 5. A similar trend was also observed by previous researchers using microchannel reactor [26,48]. As the flow rate of the MEA solution increases, the ultrasound exposure time inside the microreactor decreases, and consequently less received ultrasonic energy by the unit mass of MEA solution.

Generally, the violent bursting of cavitation bubbles causes the break of laminar sublayer, resulting in the increased turbulence inside the exposed liquid, so it is expected to enhance the mass transfer considerably. Ultrasound-induced turbulence, however, loses significance at larger flow rates as convection-induced turbulence, on the other hand, becomes more pronounced.

Desorption rate against concentration at various flow rates of MEA solution is plotted in Fig. 6. At the whole range of flow rate, the rate of  $\text{CO}_2$  stripping presented an increase as the MEA concentration was increased. At higher MEA concentrations, the amount of MEA as active sites for  $\text{CO}_2$  absorption is higher and naturally the solution is saturated with more amount of  $\text{CO}_2$ , therefore during amine solvent regeneration process it has more  $\text{CO}_2$  for desorption.

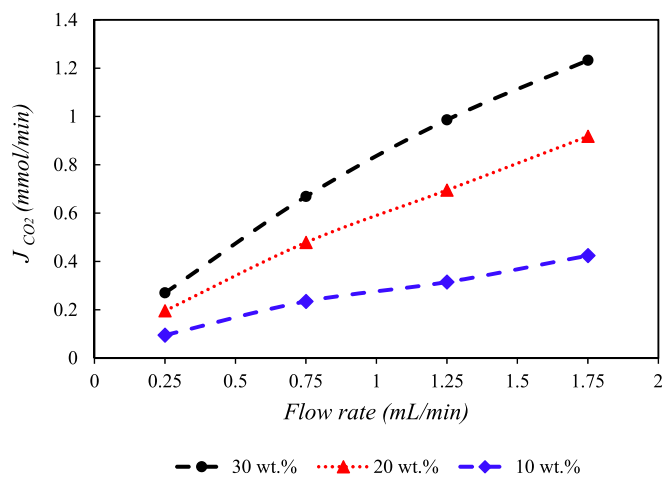


Fig. 4. Effects of flow rate and MEA concentration on CO<sub>2</sub> desorption rate.

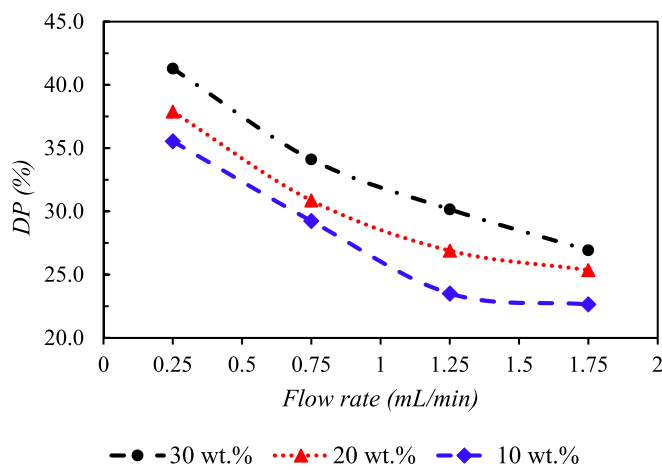


Fig. 5. Effects of flow rate and concentration of MEA solution on desorption percentage at maximum ultrasound power.

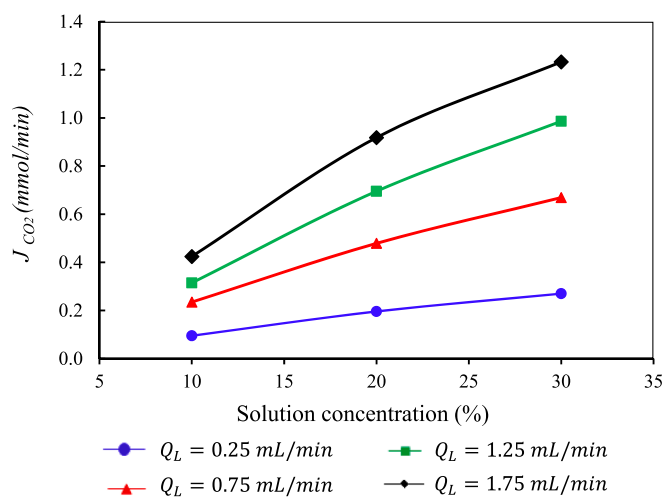


Fig. 6. Effects of MEA solution concentration on desorption rate at maximum ultrasound power.

#### The effect of temperature

As previously mentioned, CO<sub>2</sub> desorption process from MEA solution was performed in the range of 55–85 °C, which was considered lower

than temperatures applied to the conventional methods in order to reduce the degradation. CO<sub>2</sub> desorption percentage from 30 wt% MEA solution at various flow rates as a function of the temperature is depicted in Fig. 7, indicating an increasing trend. Such an upward trend was obtained by Aghel et al. [48]. As the temperature increases, the respective equilibrium CO<sub>2</sub> loading get decreased. Therefore, at lower temperature, there is a small difference between equilibrium and initial CO<sub>2</sub> loadings, resulting in a slight driving force for gas–liquid mass transfer, hence, the desorption percentage get decreased.

#### The effect of ultrasound power

The amount of power which is imparted to the targeted fluid is an important characteristics of ultrasonic waves. 100 % and 0 % power amplitudes determine, respectively, the rated ultrasonication power and the condition without ultrasonic propagation [49]. Ultrasound intensity, the average power per unit cross-sectional area perpendicular to acoustic radiation direction, expresses the strength of vibrations [50]. The ultrasonic intensity strongly causes an increase heat and mass transfer through disruption of the boundary layers [51]. Whereas the ultrasound power has shown a significant effect on different ultrasound-assisted processes, the influence of this parameter was also assessed in the present investigation. The effect of different ultrasonic amplitudes (40, 60, 80, 100 %) on desorption rate of CO<sub>2</sub> is presented in Fig. 8, indicating direct association between ultrasound power and desorption rate. This concept can be explained by the direct relationship between the intensity of the cavitation bubbles implosion and the ultrasound power. The ultrasonic power is directly proportional to the size of the acoustic cavitation bubbles. Therefore, with increasing the ultrasound power, some effects which are induced by implosion are also resonated. This enhances mixing through the liquid medium and consequently leads to an increase in the mass transfer rate. Although, an increase in ultrasound power resulted in enhancement of CO<sub>2</sub> desorption rate at the whole flow rate range, the changes were insignificant for flow rate of 0.25 mL/min. Regarding to very low flow rate, the amount of rich MEA solution and consequently CO<sub>2</sub> gas passing through the microchannel during the experiment was also low, thereby the change in its amount was not considerable even at maximum ultrasound power.

For evaluation of ultrasound power effects, it is conceptual to discuss the desorption percentage demonstrated in Fig. 9. Desorption percentage increased with increasing the ultrasound power at all flow rates, however amounts of this parameter at flow rate of 0.25 mL/min was much greater than others because of having longer retention time. The velocity of the solution inside a microchannel with a lower flow rate get reduced. Lower velocity led to larger retention time of the solution inside the microchannel so that the solution traveled a longer time at

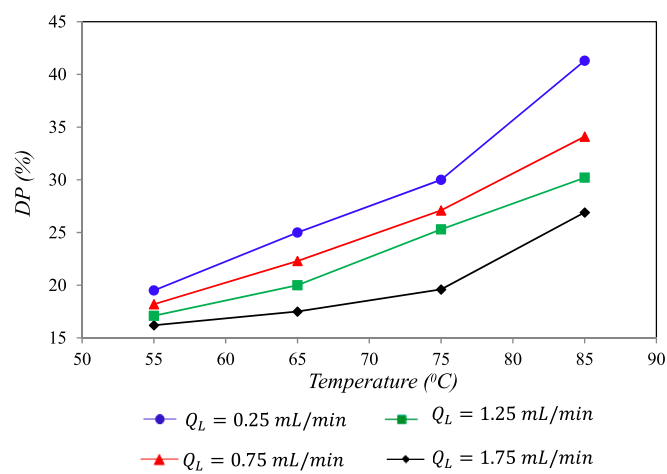


Fig. 7. Effect of temperature on desorption percentage at maximum ultrasound power.

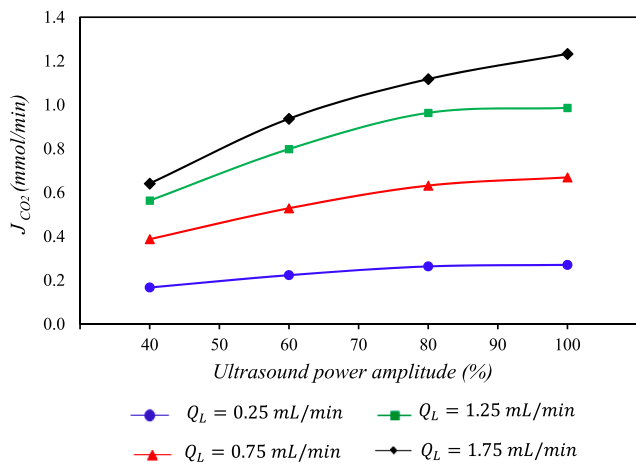


Fig. 8. Effect of ultrasound power on desorption rate for 30 wt% MEA solution.

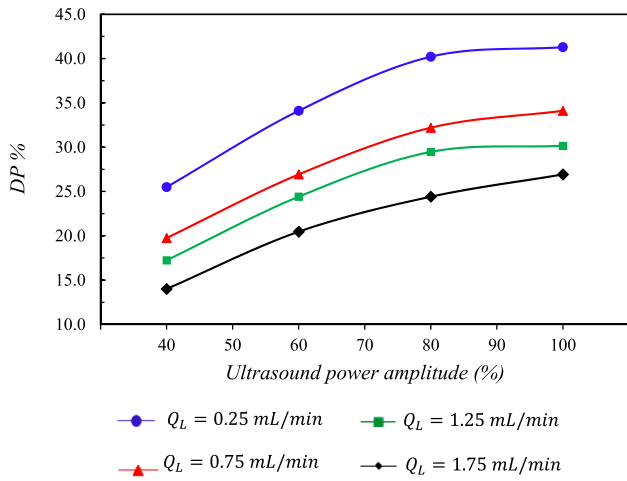


Fig. 9. Effect of ultrasound power on desorption percentage for 30 wt% MEA solution.

desorption temperature, and this increased the possibility of  $CO_2$  desorption. Also for the lowest flow rate, a reduction in slope of the graph was observed with increased ultrasound power. This is due to the intensification of heating effect at higher intensities of ultrasound. In addition to improving the mass transfer, ultrasonication generates some heat inside the MEA solution due to the collapse of the acoustic cavitation bubbles, particularly at high power amplitudes. Hence, the beneficial influence of ultrasonic vibrations on gas–liquid mass transfer, subsequently, on  $CO_2$  desorption steadily decreases at larger power amplitudes.

#### Energy analysis

Evaluation of the energy needed to desorb a unit mass of  $CO_2$  is a critical issue in studies on  $CO_2$  stripping.  $E_{des}$  was obtained using Eq. (9).

Desorption energy consumption per unit mass of  $CO_2$  as a function of ultrasound power amplitude for MEA solution with different concentrations is depicted in Fig. 10. Desorption energy consumption increased by almost 3 times when MEA concentration decreases from 30 wt% to 10 wt%. At higher MEA concentration, more  $CO_2$  passed through the microchannel in a specific time and flow rate, so ultrasound energy received by the solution was expended on separating more amount of  $CO_2$  compared to the lower concentration. Therefore, in order to reach higher energy saving, it is advantageous to use the designed contactor for  $CO_2$  stripping from MEA solution with high concentration.

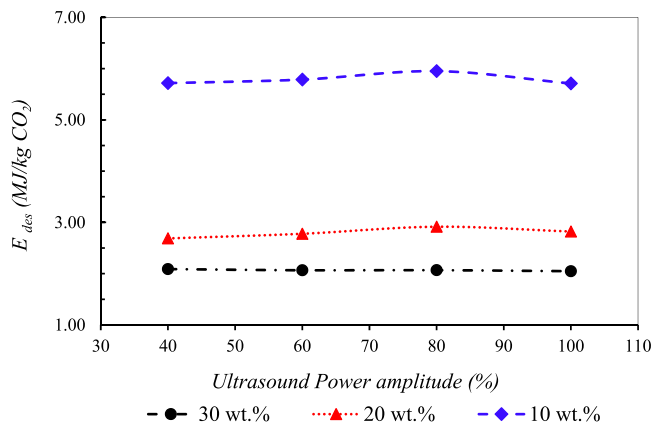


Fig. 10. Effects of MEA concentration and ultrasound power on desorption energy consumption for MEA solution with flow rate of 0.25 mL/min.

The impact of ultrasound power and flow rate of MEA solution with concentration of 30 wt% is illustrated in Fig. 10 and Fig. 11. As is clear from Fig. 10 and Fig. 11, ultrasound power, represented no considerable influence on desorption energy consumption at lower flow rates. Desorption energy consumption indicated an increasing trend with increasing the flow rate in the entire range of ultrasound power, demonstrating that the increase in the gained energy by the MEA solution was higher than the increase in the amount of separated  $CO_2$  as the MEA solution flow rate rose. Whereas at low flow rate, desorption energy consumption was almost not affected by ultrasound power, while its associated desorption percentage was higher, it can be concluded that the sono-microreactor could work as a highly effective contactor for  $CO_2$  desorption from MEA solution at lower flow rates. For 30 wt% MEA solution,  $E_{des}$  was reported 4.2 MJ/kg  $CO_2$  as an standard value for conventional methods [38]. At the lowest flow rate of 30 wt% MEA solution, this parameter was obtained 2 MJ/kg  $CO_2$  employing the designed ultrasound-equipped microreactor, indicating 52.3 % energy saving.

Therefore, as a novel technique for  $CO_2$  stripping which is performed at lower temperatures than traditional methods, the contactor performance seems great. Low-temperature  $CO_2$  desorption can lessen solvent degradation. Solvent degradation is an unfavorable consequence of using high temperature in amine-based  $CO_2$  desorption processes; it causes higher costs as well as formation of adverse products. MEA degradation is strongly affected by the temperature so that a 17 °C decrease in the temperature causes 4-fold reduction of MEA degradation [52]. Therefore, ultrasound, which provides the required energy of the  $CO_2$  desorption process at low temperature, may considered as an advantageous technique. It can be said that direct touch of microchannel with acoustic vibrations, which results in higher power gained by the unit volume of the passing solution, is the significant strength of the developed contactor.

#### $CO_2$ desorption from aqueous blended AMP/MEA solutions

Sterically hindered amines are a group of chemical absorbents which has been proposed for  $CO_2$  capture due to some merits including high absorption rate and capacity, high resistance to degradation, and low regeneration energy consumption [53]. One of the most popular sterically hindered amines is 2-amino-2-methyl-1-propanol (AMP). On the other hand, mixtures of alkanolamines have not only shown improved absorption characteristics but also upgraded stripping characteristics such as reducing regeneration energy demand. Although some studies have focused on evaluating the behavior of blended amine solutions containing AMP [44,53,54], regeneration process and its associated energy requirement have rarely studied by the researchers.

Therefore, in the present study, two different MEA/AMP blending ratios of 2/1 and 1/2 in aqueous 30 wt% solution were also evaluated.

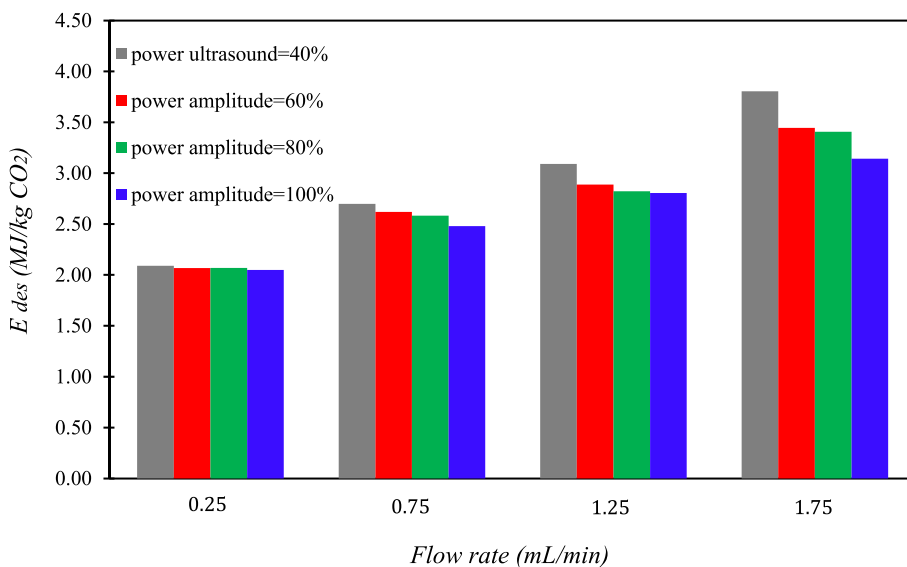


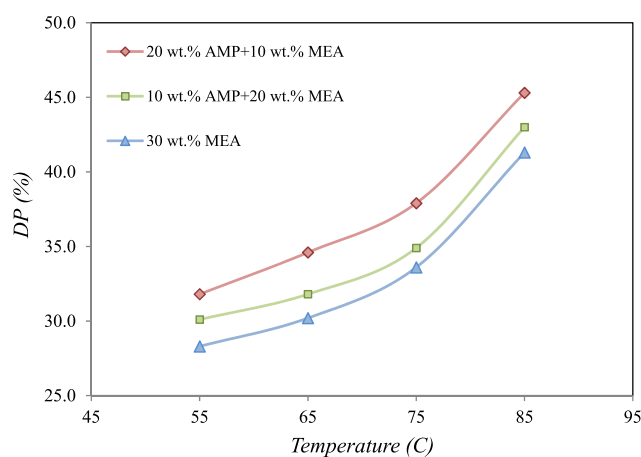
**Fig. 11.** Effects of flow rate and ultrasound power on desorption energy consumption for MEA solution with concentration of 30 wt%.

The aim was to compare two blends of MEA and AMP, one of which had a higher concentration of MEA and the other had a higher concentration of AMP.  $\text{CO}_2$  desorption percentage for blends of AMP and MEA at different temperatures is displayed in Fig. 12.

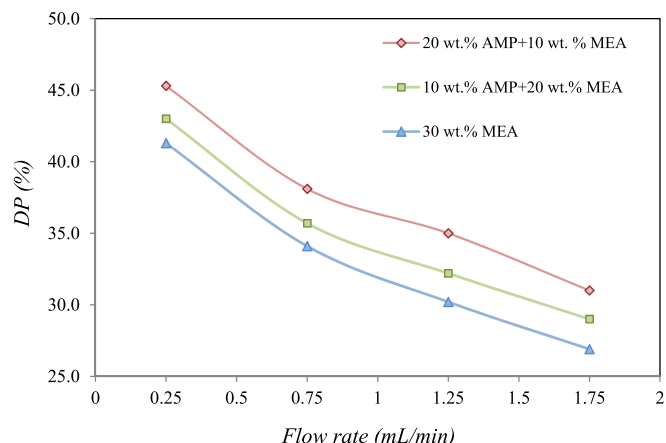
As found from this figure, desorption percentage of MEA solution increased when it mixed with AMP. 20 wt% AMP + 10 wt% MEA showed the maximum desorption percentage, indicating 9.6 % increase compared to 30 wt% MEA at 85 °C. As 30 wt% MEA solution, an increasing trend with increase in temperature was also observed for both mixtures due to growing the driving force of the mass transfer.

Fig. 13 illustrates  $\text{CO}_2$  desorption percentage for blends of AMP and MEA versus flow rates of the solution, indicating expected downward trend as 30 wt% MEA.

$E_{des}$  for AMP/MEA mixture versus flow rate is shown in Fig. 14. The minimum values of regeneration energy in the range of 1.6–2.3  $\text{MJ}/\text{kg CO}_2$  was obtained for the case of 20 wt% AMP + 10 wt% MEA. It can be attributed to the higher absorption capacity of AMP than normal alkanolamines, so the solution containing more AMP has more amount of  $\text{CO}_2$  for desorption. In addition, the heat of absorption for AMP is 28 % lower than that for 30 wt% MEA [54]. The results also illustrated approximately 62 % energy reduction compared to 30 wt% MEA benchmark in traditional method for 20 wt% AMP + 10 wt% MEA solution at 0.25  $\text{mL}/\text{min}$ .



**Fig. 12.** Desorption percentage of AMP/MEA mixture versus temperature.



**Fig. 13.** Desorption percentage of AMP/MEA mixture versus flow rate.

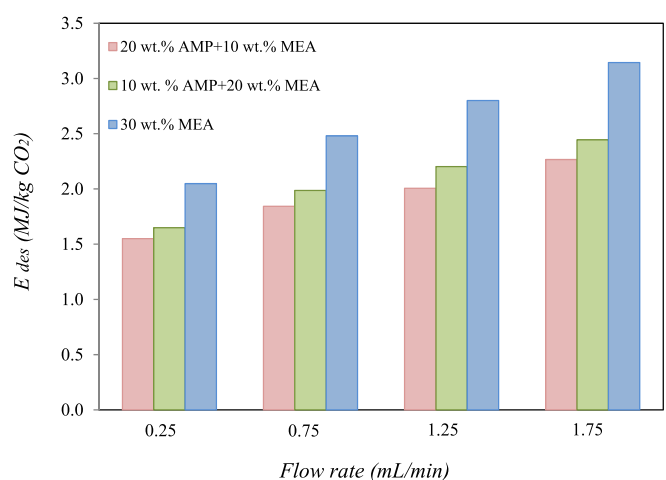


**Fig. 14.** Desorption energy consumption of AMP/MEA mixture at different flow rates.

## Conclusions

$\text{CO}_2$  desorption from the aqueous amine solutions using a novel and efficient contactor was experimentally investigated. A long micro-tube was placed in the direct touch with ultrasonic transducer without the existence of a liquid medium. In addition, no heat was applied to the sono-microreactor. The behavior of two-phase flow was evaluated using a digital microscope camera, illustrating the formation of gas bubbles and its growing as a result of mass transfer through the contactor. It was concluded that the simultaneous use of ultrasound and microchannel reactor, each of them has unique effects on mass transfer enhancement, could lead to intensification of  $\text{CO}_2$  desorption. First, MEA as a benchmark solvent was studied. The influence of MEA concentration, flow rate of the loaded MEA solution, temperature, and ultrasound power on the rate and percentage of desorption was studied. With increasing the flow rate, desorption percentage showed a decrease, while it indicated an increase with increasing temperature, ultrasound power and concentration of MEA solution. Energy analysis was also performed, demonstrating 52.3 % energy saving compared to the conventional technique. Also, aqueous 30 wt% MEA/AMP solutions with two different blending ratios of 2/1 and 1/2 were evaluated. Approximately 62 % energy saving compared to 30 wt% MEA benchmark in conventional method was reached for 20 wt% AMP + 10 wt% MEA solution at 0.25 mL/min.

## CRediT authorship contribution statement

**Hamed Rashidi:** Conceptualization, Methodology, Writing - review & editing, Supervision, Project administration. **Maryam Dehbani:** Writing- original draft preparation, Validation, Formal analysis, Investigation. **Mahyar Amiri:** Validation, Investigation.

## Declaration of competing interest

The authors declare that they have no known competing financial interests or personal relationships that could have appeared to influence the work reported in this paper.

## References

- [1] X. Zhang, et al., Reducing energy consumption of  $\text{CO}_2$  desorption in  $\text{CO}_2$ -loaded aqueous amine solution using  $\text{Al}_2\text{O}_3/\text{HZSM-5}$  bifunctional catalysts, *Applied Energy* 229 (2018) 562–576.
- [2] A.S. Bairq, Z., et al., Enhancing  $\text{CO}_2$  desorption performance in rich MEA solution by addition of  $\text{SO}_4^{2-}/\text{ZrO}_2/\text{SiO}_2$  bifunctional catalyst, *Applied Energy* 252 (2019) 113440.
- [3] M. Aghaie, N. Rezaei, S. Zendehboudi, A systematic review on  $\text{CO}_2$  capture with ionic liquids: Current status and future prospects, *Renewable and Sustainable Energy Reviews* 96 (2018) 502–525.
- [4] K. Li, et al., Systematic study of aqueous monoethanolamine-based  $\text{CO}_2$  capture process: model development and process improvement, *Energy Science & Engineering* 4 (1) (2016) 23–39.
- [5] X. Zhang, et al., Evaluating  $\text{CO}_2$  desorption performance in  $\text{CO}_2$ -loaded aqueous tri-solvent blend amines with and without solid acid catalysts, *Applied Energy* 218 (2018).
- [6] P. Valeh-e-Sheyda, J. Barati, Mass transfer performance of carbon dioxide absorption in a packed column using monoethanolamine-Glycerol as a hybrid solvent, *Process Safety and Environmental Protection* 146 (2021) 54–68.
- [7] X. Zhang, et al., Reduction of energy requirement of  $\text{CO}_2$  desorption from a rich  $\text{CO}_2$ -loaded MEA solution by using solid acid catalysts, *Applied Energy* 202 (C) (2017) 673–684.
- [8] C.-H. Cheng, et al., Amine-based post-combustion  $\text{CO}_2$  capture mediated by metal ions: Advancement of  $\text{CO}_2$  desorption using copper ions, *Applied Energy* 211 (2018) 1030–1038.
- [9] G.T. Rochelle, Thermal degradation of amines for  $\text{CO}_2$  capture, *Current Opinion in Chemical Engineering* 1 (2) (2012) 183–190.
- [10] A.B. Rao, E.S. Rubin, A Technical, Economic, and Environmental Assessment of Amine-Based  $\text{CO}_2$  Capture Technology for Power Plant Greenhouse Gas Control, *Environmental Science & Technology* 36 (20) (2002) 4467–4475.
- [11] S.C. Tiwari, et al., A strategy of development and selection of absorbent for efficient  $\text{CO}_2$  capture: An overview of properties and performance, *Process Safety and Environmental Protection* 163 (2022) 244–273.
- [12] M. Zhang, Y. Guo, Analysis on Regeneration Energy of  $\text{NH}_3$ -based  $\text{CO}_2$  Capture with Equilibrium-based Simulation Method, *Energy Procedia* 114 (2017) 1480–1487.
- [13] B. Zhang, et al., Evaluating  $\text{CO}_2$  Desorption Activity of Tri-Solvent MEA + EAE + AMP with Various Commercial Solid Acid Catalysts, *Catalysts* 12 (2022), <https://doi.org/10.3390/catal12070723>.
- [14] H. Rashidi, P. Valeh-e-Sheyda, S. Sahraie, A multiobjective experimental based optimization to the  $\text{CO}_2$  capture process using hybrid solvents of MEA-MeOH and MEA-water, *Energy* 190 (2020) 116430.
- [15] H. Rashidi, S. Sahraie, Enhancing carbon dioxide absorption performance using the hybrid solvent: Diethanolamine-methanol, *Energy* 221 (2021) 119799.
- [16] M. Pasha, et al.,  $\text{CO}_2$  absorption with diamine functionalized deep eutectic solvents in microstructured reactors, *Process Safety and Environmental Protection* 159 (2022) 106–119.
- [17] F. Liu, et al., Sustainable ionic liquid organic solution with efficient recyclability and low regeneration energy consumption for  $\text{CO}_2$  capture, *Separation and Purification Technology* 275 (2021) 119123.
- [18] M. Akbari, P. Valeh-e-Sheyda,  $\text{CO}_2$  equilibrium solubility in and physical properties for monoethanolamine glycinate at low pressures, *Process Safety and Environmental Protection* 132 (2019) 116–125.
- [19] S. Sarlak, P. Valeh-e-Sheyda, The contribution of L-Arginine to the mass transfer performance of  $\text{CO}_2$  absorption by an aqueous solution of methyl diethanolamine in a microreactor, *Energy* 239 (2022) 122349.
- [20] M. Kashid, L. Kiwi, Quantitative Prediction Of Flow Patterns In Liquid-Liquid Flow In Micro-Capillaries, *Chemical Engineering and Processing: Process Intensification* 50 (2011) 972–978.
- [21] P. Valeh-e-Sheyda, et al., An insight on reducing the particle size of poorly-water soluble curcumin via LASP in microchannels, *Chemical Engineering and Processing: Process Intensification* 91 (2015) 78–88.
- [22] M.N. Kashid, A. Renken, L. Kiwi-Minsker, Gas-liquid and liquid-liquid mass transfer in microstructured reactors, *Chemical Engineering Science* 66 (17) (2011) 3876–3897.
- [23] P. Asgarifard, M. Rahimi, N. Tafreshi, Response surface modelling of  $\text{CO}_2$  capture by ammonia aqueous solution in a microchannel. The, *Canadian Journal of Chemical Engineering* 99 (2020).
- [24] H. Rashidi, P. Rasouli, H. Azimi, A green vapor suppressing agent for aqueous ammonia carbon dioxide capture solvent: Microcontactor mass transfer study, *Energy* (2021) 122711.
- [25] H. Rashidi, M. Sahraei, Investigation of carbon dioxide absorption process in a microreactor by potash-glycerol hybrid solvent, *Journal of Separation Science and Engineering* 13 (2) (2022) 52–60.
- [26] H. Liu, et al., Desorption of carbon dioxide from aqueous MDEA solution in a microchannel reactor, *Chemical Engineering Journal* 307 (2017) 776–784.
- [27] H. Liu, et al., Heat Transfer Characteristics of  $\text{CO}_2$  Desorption from N-Methyldiethanolamine Solution in a Microchannel Reactor, *Chemical Engineering & Technology* 41 (7) (2018) 1398–1405.
- [28] M. Singla, N. Sit, Application of ultrasound in combination with other technologies in food processing: A review, *Ultrasonics Sonochemistry* 73 (2021) 105506.
- [29] M. Ja'fari, S.L. Ebrahimi, M.R. Khosravi-Nikou, Ultrasound-assisted oxidative desulfurization and denitrogenation of liquid hydrocarbon fuels: A critical review, *Ultrasonics Sonochemistry* 40 (2018) 955–968.
- [30] N. Bhargava, et al., Advances in application of ultrasound in food processing: A review, *Ultrasonics Sonochemistry* 70 (2021) 105293.
- [31] Y. Zhang, N. Abatzoglou, Review: Fundamentals, applications and potentials of ultrasound-assisted drying, *Chemical Engineering Research and Design* 154 (2020) 21–46.
- [32] G. Guo, et al., Enhanced porosity and permeability of three-dimensional alginate scaffolds via acoustic microstreaming induced by low-intensity pulsed ultrasound, *Ultrasonics Sonochemistry* 37 (2017) 279–285.
- [33] J. Jalal, T.S.H. Leong, Microstreaming and Its Role in Applications: A Mini-Review, *Fluids* 3 (4) (2018) 93.
- [34] W.H. Tay, K.K. Lau, A.M. Shariff, High frequency ultrasonic-assisted  $\text{CO}_2$  absorption in a high pressure water batch system, *Ultrasonics Sonochemistry* 33 (2016) 190–196.
- [35] S. Gantert, D. Möller, Ultrasonic Desorption of  $\text{CO}_2$  – A New Technology to Save Energy and Prevent Solvent Degradation, *Chemical Engineering & Technology* 35 (2012).
- [36] K. Tanaka, et al., Ultrasound irradiation for desorption of carbon dioxide gas from aqueous solutions of monoethanolamine, *Japanese Journal of Applied Physics* 53 (7S) (2014) p. 07KE14.
- [37] J. Ying, et al., Ultrasound intensified  $\text{CO}_2$  desorption from pressurized loaded monoethanolamine solutions. I. parameters investigation and modelling, *Energy* 163 (2018).
- [38] J. Ying, et al., Ultrasound intensify  $\text{CO}_2$  desorption from pressurized loaded monoethanolamine solutions, II. Optimization and Cost Estimation. *Energy* 173 (2019) 218–228.
- [39] B. Ahmed-Omer, D. Barrow, T. Wirth, Effect of segmented fluid flow, sonication and phase transfer catalysis on biphasic reactions in capillary microreactors, *Chemical Engineering Journal* 135 (2008) S280–S283.
- [40] S. Aljbour, H. Yamada, T. Tagawa, Ultrasound-assisted phase transfer catalysis in a capillary microreactor, *Chemical Engineering and Processing: Process Intensification* 48 (2009) 1167–1172.
- [41] D. Fernandez Rivas, P. Cintas, H.J.G.E. Gardeniers, Merging microfluidics and sonochemistry: towards greener and more efficient micro-sono-reactors, *Chemical Communications* 48 (89) (2012) 10935–10947.
- [42] D. Fernandez Rivas, S. Kuhn, Synergy of Microfluidics and Ultrasound, *Topics in Current Chemistry* 374 (5) (2016) 70.
- [43] W. Horwitz, Association of Official Analytical Chemists (AOAC), *Methods*. (1975).

- [44] W.-J. Choi, et al., Removal characteristics of CO<sub>2</sub> using aqueous MEA/AMP solutions in the absorption and regeneration process, *Journal of Environmental Sciences* 21 (7) (2009) 907–913.
- [45] K. Kumar, S. Srivastav, V.S. Sharanagat, Ultrasound assisted extraction (UAE) of bioactive compounds from fruit and vegetable processing by-products: A review, *Ultrasonics Sonochemistry* 70 (2021) 105325.
- [46] J.J. John, et al., Ultrasound assisted liquid–liquid extraction in microchannels—A direct contact method, *Chemical Engineering and Processing: Process Intensification* 102 (2016) 37–46.
- [47] Uchida, T. and T. Kikuchi, *Ultrasonic power measurement by calorimetric method using water as heating material Investigation on thermal effects other than ultrasound*. 2013. 1657-1660.
- [48] B. Aghel, S. Sahraie, E. Heidaryan, Comparison of aqueous and non-aqueous alkanolamines solutions for carbon dioxide desorption in a microreactor, *Energy* 201 (2020) 117618.
- [49] M. Palma, C.G. Barroso, Ultrasound-assisted extraction and determination of tartaric and malic acids from grapes and winemaking by-products, *Analytica Chimica Acta* 458 (1) (2002) 119–130.
- [50] *Diagnostic Radiology Physics*. 2014, Vienna: INTERNATIONAL ATOMIC ENERGY AGENCY.
- [51] K. Viriyananon, et al., Characterization of heat transfer and friction loss of water turbulent flow in a narrow rectangular duct under 25–40 kHz ultrasonic waves, *Ultrasonics* 114 (2021) 106366.
- [52] J. Davis, G. Rochelle, Thermal degradation of monoethanolamine at stripper conditions, *Energy Procedia* 1 (1) (2009) 327–333.
- [53] B.P. Mandal, S.S. Bandyopadhyay, Absorption of carbon dioxide into aqueous blends of 2-amino-2-methyl-1-propanol and monoethanolamine, *Chemical Engineering Science* 61 (16) (2006) 5440–5447.
- [54] Y. Kim, et al., Comparison of carbon dioxide absorption in aqueous MEA, DEA, TEA, and AMP solutions, *Bulletin of the Korean Chemical Society* 34 (2013).